

HUNTING THE NATURE OF IGR J17497–2821 WITH X-RAY AND NIR OBSERVATIONS

A. PAIZIS¹, M. A. NOWAK², S. CHATY³, J. RODRIGUEZ³, T. J.-L. COURVOISIER^{4,5}, M. DEL SANTO⁶, K. EBISAWA⁷, R. FARINELLI⁸, P. UBERTINI⁶, AND J. WILMS⁹

Draft version May 25, 2019

ABSTRACT

We report on a *Chandra* grating observation of the recently discovered hard X-ray transient IGR J17497–2821. The observation took place about two weeks after the source discovery at a flux level of about 20 mCrab in the 0.8–8 keV range. We extracted the most precise X-ray position of IGR J17497–2821, $\alpha_{J2000}=17^h 49^m 38^s.037$, $\delta_{J2000}=-28^\circ 21' 17''.37$ (90% uncertainty of $0''.6$). We also report on optical and near infra-red photometric follow-up observations based on this position. With the multi-wavelength information at hand, we discuss the possible nature of the source proposing that IGR J17497–2821 is a low-mass X-ray binary, most likely hosting a black hole, with a red giant K-type companion.

Subject headings: X-rays: binaries – binaries: close – stars: individual: IGR J17497–2821

1. INTRODUCTION

On 2006 September 17 a new hard-X ray transient, IGR J17497–2821 (Soldi et al. 2006), was discovered by the IBIS telescope (Ubertini et al. 2003) on-board *INTEGRAL* (Winkler et al. 2003). The source was first detected at a flux of about 25 mCrab in the 20–40 keV range and further observations (Shaw et al. 2006; Kuulkers et al. 2006) indicated that IGR J17497–2821 was brightening with a 3–200 keV *INTEGRAL* spectrum well fitted by an absorbed power-law with $\Gamma=1.93\pm 0.05$. Two days later, a *Swift* observations was performed and a *Swift*/XRT position at $\alpha_{J2000}=17^h 49^m 38^s.1$, $\delta_{J2000}=-28^\circ 21' 16''.9$ with uncertainty of $5''.3$ radius (90% containment) was reported (Kennea et al. 2006). The XRT spectrum was well fitted using an absorbed power-law with $N_H=(4.8 \pm 0.3)\times 10^{22}$ cm⁻² and $\Gamma=1.6 \pm 0.1$. The source was also detected by *RXTE*/PCA (Markwardt & Swank 2006) and *Suzaku* (Itoh et al. 2006). In the quest to understand the nature of this new transient, archival optical and follow-up Near Infra-Red (NIR) observations were reported (Laycock et al. 2006; Chaty et al. 2006a,b, respectively). Nevertheless, the location of the source near the Galactic center made it very difficult to assess a unique optical-NIR identification and a sub-arcsec accuracy of the X-ray source was clearly needed (Paizis et al.

2006; Torres et al. 2006). In this letter we present a *Chandra* grating observation of IGR J17497–2821 together with optical-NIR observations¹⁰ based on the X-ray position (sub-arcsec accuracy) obtained with our *Chandra* data.

2. OBSERVATIONS AND DATA ANALYSIS

2.1. *Chandra* data

We observed IGR J17497–2821 for 19 ksec with *Chandra* on 2006 October 1 from 17:42 UT until 23:42 UT (MJD 54010). The High Energy Transmission Grating Spectrometer, HETGS (Canizares et al. 2000), was used. It has two sets of gratings, the High Energy Grating, HEG 0.8–10 keV, and Medium Energy Grating, MEG 0.4–8.0 keV. We reduced the data in a standard manner, using the CIAO version 3.3 software package and *Chandra* CALDB version 3.2.3. The spectra were analyzed with the ISIS analysis system, version 1.3.0 (Houck 2002). We obtained the X-ray position of the source using the *findzero.sl* routine¹¹, strongly recommended by the *Chandra* grating team in case of bright sources for which the zeroth-order (un-dispersed) position is piled-up (about 47% pile-up in the present case). We extracted the first order dispersed spectra ($m = \pm 1$ for HEG and MEG, for a total of four spectra) and to increase the signal-to-noise ratio, we merged the two HEG ($m = \pm 1$) and MEG ($m = \pm 1$) spectra into two final combined spectra. We binned the data to obtain a minimum of 16 counts per bin for both HEG and MEG (0.8–8 keV), as well as a minimum number of 16 channels per bin for HEG and 8 for MEG.

2.2. *Optical and NIR data*

We also obtained optical photometry in *U* (357.08 nm), *B* (421.20 nm), *V* (544.17 nm), *R* (641.58 nm), *I* (794.96 nm) and *Z* (840.90 nm) bands of the field of view of IGR J17497–2821 with the imager SUSI2, installed on the 3.5 m New Technology Telescope (NTT) of La Silla

Electronic address: ada@iasf-milano.inaf.it

¹ IASF Milano - INAF, Via Bassini 15, 20133 Milano, Italy

² Center for Space Research, MIT, Cambridge, MA, USA

³ AIM - Astrophysique Interactions Multi-échelles (UMR 7158 CEA/CNRS/Université Paris 7 Denis Diderot) CEA Saclay, DSM/DAPNIA/Service d'Astrophysique, FR-91 191 Gif-sur-Yvette Cedex, France

⁴ *INTEGRAL* Science Data Centre, Chemin d'Ecogia 16, 1290 Versoix, Switzerland

⁵ Observatoire de Genève, 51 chemin des Mailletes, 1290 Sauverny, Switzerland

⁶ IASF Roma - INAF, Via del Fosso del Cavaliere 100, 00133 Roma, Italy

⁷ ISAS 3-1-1 Yoshinodai, Sagamihara, Kanagawa 229-8510, Japan

⁸ Dipartimento di Fisica, Università di Ferrara, Via Saragat 1, I-44100 Ferrara, Italy

⁹ Dr. Karl Remeis-Sternwarte, Astronomisches Institut, Universität Erlangen-Nürnberg, Sternwartstr. 7, 96049 Bamberg, Germany

¹⁰ The optical and NIR observations were obtained as part of the European Southern Observatory (ESO) Target of Opportunity program 078.D-0268 (PI S. Chaty).

¹¹ <http://space.mit.edu/CXC/analysis/findzo/index.html>

observatory (ESO, Chile). The observations were performed on 2006 October 3 between 00:01 UT and 00:12 UT and 2006 October 7 between 23:55 UT and 8 00:06 UT. We used the large field imaging of SUSI2's detector with $0''.166 \text{ pixel}^{-1}$ image scale and $5'.5 \times 5'.5$ field of view (FoV). The images were binned by a factor 2, and the integration time was of 60s for each exposure. Photometry was preformed relative to the standard star Mark-A of Landolt (1992).

We also obtained NIR photometry in J ($1.247 \mu\text{m}$), H ($1.653 \mu\text{m}$) and K_s ($2.162 \mu\text{m}$) bands of the field around IGR J17497–2821 with the spectro-imager SofI, installed on the NTT. The observations were performed in two epochs, the first between 2006 October 1, 23:48 UT, and October 2, 00:11 UT, and the second between October 3, 23:45 UT, and October 4, 00:09 UT. We used the large field imaging of SofI's detector with $0''.288 \text{ pixel}^{-1}$ image scale and a $4'.94 \times 4'.94$ FoV. To accurately determine the sky brightness, the observations consisted of nine slightly ($30''$) dithered frames of 10 sec each per filter, for a total exposure of 90sec in each filter. Photometry was preformed relative to the standard stars sj9181 and sj9183 of Persson et al. (1998).

We used the Image Reduction and Analysis Facility (IRAF) suite to perform data reduction, carrying out standard procedures of optical and NIR image reduction. Aperture photometry in the crowded field of IGR J17497–2821 was performed with the daophot package of the IRAF suite. This package allows one to build a synthetic Point Spread Function (PSF) using bright and isolated stars in the field of view, and then to scale and subtract this PSF from all the stars. With an iterative PSF subtraction it is possible to reveal fainter objects which are hidden in the glare of brighter ones, such as blended objects.

3. RESULTS

A hard X-ray intensity history of the 2006 outburst of IGR J17497–2821 seen by *Swift*/BAT is presented in Fig. 1, left panel. The time of our *Chandra*, optical and NIR observations are shown by the indicated arrows.

3.1. X-ray position and grating spectrum

We extracted the X-ray position of IGR J17497–2821 from the zeroth-order image obtaining $\alpha_{J2000}=17^h 49^m 38^s.037$, $\delta_{J2000}=-28^\circ 21' 17''.37$. Given the brightness of the source, the statistical error is smaller than the absolute position accuracy of *Chandra*, $0''.6$ at 90% uncertainty¹². Therefore we attribute to the position found a 90% uncertainty of $0''.6$. This position, compatible with the *Swift*/XRT one (Kennea et al. 2006), was immediately announced to the community by Paizis et al. (2006). The first order HEG and MEG spectra of IGR J17497–2821 are shown in Fig. 1, right panel. An absorbed power-law with column density $N_{\text{H}}=(4.4 \pm 0.1) \times 10^{22} \text{ cm}^{-2}$ (PHABS model) and photon index $\Gamma = 1.23 \pm 0.05$ fits the data with a reduced $\chi^2_{\nu}=1.17$ for 335 d.o.f in the 0.8–8keV band (Table 1). The absorbed flux is about $3 \times 10^{-10} \text{ erg cm}^{-2} \text{ s}^{-1}$ in the 0.8–8keV range ($\sim 20 \text{ mCrab}$) with no discrete features evident in the spectrum, aside from the ISM absorption edges associated with Si and S (see Fig. 1, right). We

detect a hint of He-like Si absorption line at 1.867keV (Si XIII, 3σ level), likely associated to the ISM in its hot-diffuse phase. If confirmed, this is the first detection of Si in the hot ISM (Wang et al. 2005). The power-law slope of ~ 1.2 is harder than the measurements currently available from the other missions ($\Gamma = 1.6$, Kennea et al. 2006; Itoh et al. 2006; Rodriguez et al. 2006). The source is rather constant during our observation and instrumental issues such as a high pile-up are very unlikely (pile-up fraction in the HETGS arms of about 2%). Most likely, the heavy absorption of the system leaves a *Chandra* effective energy range that is very narrow (1.5-8 keV), and we are systematically underestimating both the spectral slope and the absorption column density. The power-law model alone does not seem to be the best fit model for the *Chandra* grating spectra and adding a thermal component (DISKBB) to the power-law (Γ fixed to 1.6 and then let free) results in a much better fit (probability of $\sim 10^{-7}$ that the improvement was purely due to chance). Table 1 shows the spectral parameters we obtain with the new model to which we added also a marginally detected 6.4 keV iron line ($\Delta\chi^2=9$ for the three additional line parameters).

3.2. Astrometry

We computed the astrometry of the Z and K_s band images of IGR J17497–2821, respectively taken on 2006 October 8, 00:05 UT, and 2006 October 2, 00:10 UT. The optical astrometry has been computed with all USNO stars located in the field, while the NIR astrometry used all 2MASS stars located in the field. The rms error on the astrometry is respectively of $0''.35$ for the optical image and $0''.32$ for the NIR one. The field of view of IGR J17497–2821 in the optical (Z band) and in the NIR (K_s band) are shown in Fig. 2, left and right panel respectively. We over-plot the *Swift*/XRT 90% error circle, $5''.3$ radius (Kennea et al. 2006), and the *Chandra* 90% error circle, $0''.6$ radius (this paper). The inspection of the Z image (Fig. 2, left) shows that there is no visible counterpart inside the *Chandra* 90% error circle. In the K_s band image (Fig. 2, right), inside the *Swift*/XRT error circle, there are three 2MASS sources (2MASS 17493780–2821181, 2MASS 17493774–2821173 and 2MASS 17493798–2821120, respectively labeled 2M1, 2M2 and 2M3) and some additional sources which have been labeled according to Chaty et al. (2006b). Source #1 is in fact a blended source (Torres et al. 2006). We call $1b$ the new source closest to the *Chandra* position ($0''.1$ away) and $1a$ the other one of the blend ($0''.612$ away).

3.3. Photometry

The iterative cleaning process described in Section 2.2 allowed us to extract magnitudes even for the blended objects shown in Fig. 2, right panel. The obtained instrumental magnitudes were transformed into apparent magnitudes with the standard method described in Massey & Davis (1992). There is no object detected inside the *Chandra* error circle in the optical images up to a magnitude of $V \sim 23$. Concerning the NIR, we took the images of the first epoch (2006 October 1–2) since for the images of the second epoch the conditions were not photometric, and the objects $1a$ and $1b$ could not be deblended. In the J and H images the candidate $1b$ is not

¹² <http://cxc.harvard.edu/cal/ASPECT/celmon/>

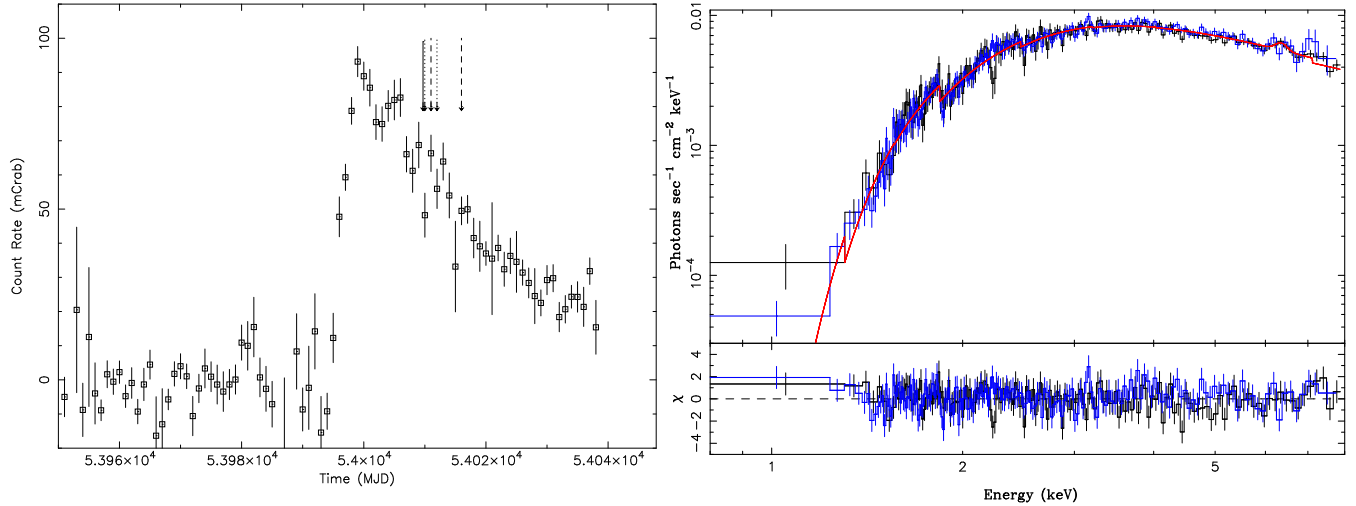


FIG. 1.— *Left panel*: X-ray intensity history of the 2006 outburst of IGR J17497–2821 (*Swift*/BAT 15–50 keV data). We also indicate the time of our follow-up observations: solid line arrow for *Chandra*, dotted for NIR and dashed for optical observations. *Right panel*: unfolded *Chandra* spectrum with best fit model (PHABS(DISKBB+PO+GAUSSIAN), Table 1) superimposed. Residuals between the model and the data in units of 1σ are shown.

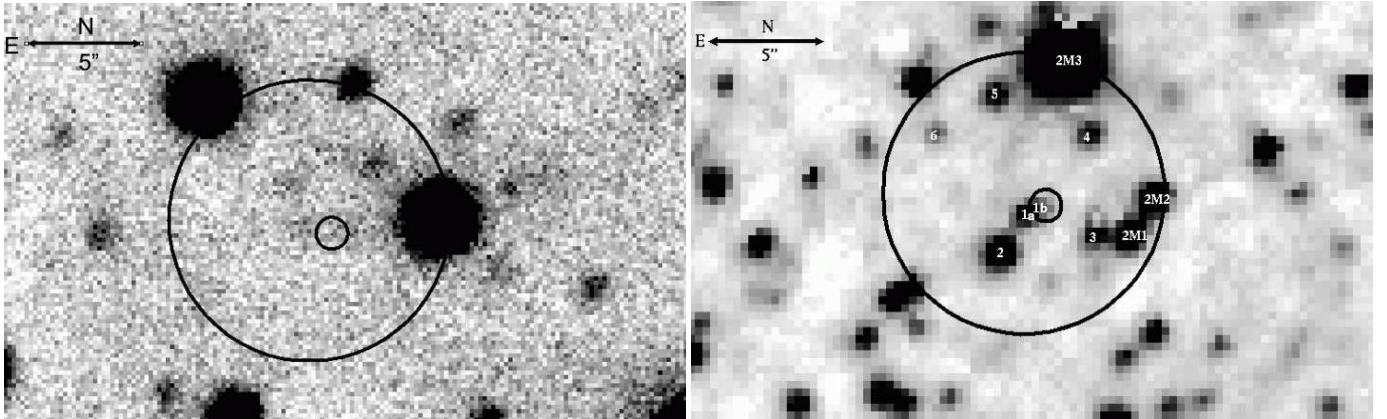


FIG. 2.— *Left panel*: Z-band image of the field of view of IGR J17497–2821. *Right panel*: K_s -band image of the field of view of IGR J17497–2821. In both images we over-plot the *Swift*/XRT 90% error circle, $5''.3$ radius (Kennea et al. 2006), and the *Chandra* 90% error circle, $0''.6$ radius (this paper). North is up, East is to the left, and the length of the arrow represents $5''$.

N_H ($\times 10^{22} \text{ cm}^{-2}$)	Γ	kT_{in} (keV)	R_{in} (km, at 8kpc)	Line_en (keV)	Line_width (keV)	Line_eq_width (eV)	$\text{Flux}_{0.8-8 \text{ keV}}$ ($\text{erg cm}^{-2} \text{ s}^{-1}$)	χ^2_{ν} (d.o.f.)
4.4 ± 0.1	1.23 ± 0.05	-	-	-	-	-	2.95×10^{-10}	1.17 (335)
5.6 ± 0.4	1.5 ± 0.1	0.19 ± 0.02	$280/\sqrt{(\cos\theta)}$	6.4 ± 0.1	< 0.22	$45.4^{+0.1}_{-32.1}$	2.90×10^{-10}	1.05 (330)

TABLE 1
SUMMARY OF THE SPECTRAL FIT PARAMETERS (0.8–8 keV).

Candidate	mag_J	mag_H	mag_{K_s}	mag_V
<i>1a</i>	20.6 ± 0.2	17.5 ± 0.2	14.7 ± 0.1	-
<i>1b</i>	-	-	16.1 ± 0.3	-
Blend <i>1a+1b</i>	-	-	-	> 23

TABLE 2
SUMMARY OF THE OPTICAL AND NIR RESULTS.

visible, therefore in Table 2 we give the apparent magnitudes of the Candidate *1a* in J and H , and the apparent magnitudes of both candidates *1a* and *1b* in K_s . The K_s magnitude of candidate *1b* is consistent with the K_s magnitude of 15.9 ± 0.2 reported by Torres et al. (2006) during observations performed ten days earlier. The source seems to be quite constant in the NIR, similarly to what

reported by Chaty et al. (2006c). There are no archival optical-NIR images of the field at the resolution achieved here so no comparison of the field before and after the X-ray outburst is possible. Follow-up observations are needed to detect any variations from candidates *1a* and *1b*, since even if candidate *1b* is the best candidate based on its proximity to the *Chandra* position, only NIR variations correlated with the X-ray flux might establish which is the real counterpart of IGR J17497–2821.

4. DISCUSSION

IGR J17497–2821 is placed in the direction of the Galactic center, $(l, b) = (0^\circ.9, -0^\circ.4)$, and we observe a column density of about $5 \times 10^{22} \text{ cm}^{-2}$ that is higher than the galactic average value expected in the source direc-

tion, $\sim 1.5 \times 10^{22} \text{ cm}^{-2}$ (Dickey & Lockman 1990). This can imply that there is an additional contribution from within the system. Nevertheless, the value obtained with the radio maps by Dickey & Lockman (1990) does not resolve the small scale non-uniformity of N_{H} and does not include the possible contribution of molecular hydrogen, probably underestimating the true value. Given the location in the sky and the high interstellar absorption, the source is most likely at the distance of the Galactic center or beyond. For our best fit model, assuming a distance of 8 kpc, we obtain an (un-absorbed) 2–10 keV source luminosity of about $4 \times 10^{36} \text{ ergs}^{-1}$, typical of X-ray binaries. The nature of the companion, *i.e.* Low Mass X-ray Binary (LMXB) versus High Mass X-ray Binary (HMXB) and of the compact object, *i.e.* Black Hole (BH) versus Neutron Star (NS) is still a matter of debate. The general X-ray properties seem to suggest that the source is a (transient) LMXB and the X-ray spectrum we obtain is compatible with a LMXB in the so-called low-hard state (LHS), cold (0.2 keV) disk emission plus power-law with $\Gamma \sim 1.5$.

Using the relation between N_{H} and interstellar extinction A_V (Predehl & Schmitt 1995) and the ratio $A_K/A_V=0.112$ (Rieke & Lebofsky 1985), our observed column density range ($4.3\text{--}6 \times 10^{22} \text{ cm}^{-2}$, to allow for both fitting models in Table 1) corresponds to a K band extinction in the range of $A_K=2.7\text{--}3.7$ magnitudes. This leads to an absolute K magnitude range of $-1.1 > M_K > -2.2$ (assumed distance of 8 kpc and observed K magnitude of $\text{mag}_K=16.1$, see Table 2). This value suggests a B-type companion, in the case of a main sequence star (therefore in a HMXB system) or a K-type companion in the case of a red giant (and then in a LMXB) (Fig. 1 in Chaty et al. 2002). We note that in the LMXB frame (favored by the X-ray properties of the source), one could envisage a scenario where the companion star is a stellar type K *main sequence* star (dimmer than the red giant K-type option) at 8 kpc that is rendered brighter by the accretion disk contribution (NIR emission from reprocessed X-rays). To obtain a main sequence K-type star from a red giant K-type star at a fixed distance we need a shift of about 6 magnitudes in M_K (Chaty et al. 2002), gap that should be covered by the disk emission alone. This is unlikely since the X-ray spectrum shows that the disk is cold

(0.2 keV) with the source being in the LHS, in which the contribution from the accretion disk is expected to be small. Conversely, in the absence of NIR disk emission, the option of a main sequence star located much closer than 8 kpc is also unlikely. In fact, the needed 6 magnitude shift would place the source as close as ~ 0.4 kpc leading to a 2–10 keV source luminosity during our *Chandra* observation of about $10^{34} \text{ ergs}^{-1}$, unusually low for a LMXB in outburst. The synergy of the NIR and soft X-ray observations presented here seem to suggest that IGR J17497–2821 is a LMXB with a red giant K-type companion. However, the B-type companion in a HMXB system (even if not favored by the X-ray lightcurve) or the LMXB main sequence possibility (with proper interplay of distance and accretion disk contribution) cannot be ruled out.

Regarding the nature of the compact object we note that up to now no pulsations or type-I X-ray bursts, that would point to presence of NS in the system, have been detected (Markwardt & Swank 2006; Rodriguez et al. 2006) so no conclusive signature is currently available to infer the nature of the compact object. Our results are consistent with a cold (0.2 keV) disk around a BH of *e.g.* 10 solar masses at a distance of 8 kpc and also the power-law slope ($\Gamma \sim 1.5$) is typical of a BH in the low-hard state (Belloni 2004). However, based on our *Chandra* grating spectrum alone, we cannot rule out the NS LMXB in the LHS scenario, even if this seems rather unlikely given that IGR J17497–2821 has been detected up to ~ 300 keV (Itoh et al. 2006), which is rather hard for a NS LMXBs. Indeed, also Rodriguez et al. (2006) favor a BH as the primary, based on the *RXTE* monitoring of IGR J17497–2821, hence using different diagnostics than ours. Determining the nature of the compact object in a non-pulsating X-ray binary is one of the most intriguing questions still unresolved and IGR J17497–2821 is a good example of such a challenge.

AP thanks S. Soldi, N. Mowlavi, S. Shaw and E. Kuulkers for updates on the near real time source behavior as seen with *INTEGRAL*. AP and MN thank Tom Aldcroft for useful discussion on the *Chandra* absolute astrometry. The outburst lightcurve presented in this paper is kindly provided by the *Swift*/BAT team.

REFERENCES

- Belloni, T., 2004, Nuclear Physics B Proceedings Supplements, 132, 337
- Canizares, C. R., et al., 2000, ApJ, 539, L41
- Chaty, S., Hatano, H., Matsuoka, Y., & Nagata, T., 2006c, The Astronomer’s Telegram, 936, 1
- Chaty, S., Hatano, H., Matsuoka, Y., & Nagata, T., 2006b, The Astronomer’s Telegram, 906, 1
- Chaty, S., Matsuoka, Y., Nagata, T., & Ueda, Y., 2006a, The Astronomer’s Telegram, 897, 1
- Chaty, S., Mirabel, I. F., Goldoni, P., Mereghetti, S., Duc, P.-A., Martí, J., & Mignani, R. P., 2002, MNRAS, 331, 1065
- Dickey, J. M., & Lockman, F. J., 1990, ARA&A, 28, 215
- Houck, J. C., 2002, in High Resolution X-ray Spectroscopy with XMM-Newton and Chandra
- Itoh, T., et al., 2006, The Astronomer’s Telegram, 914, 1
- Kennea, J. A., Burrows, D. N., Nousek, J., & Gehrels, N., 2006, The Astronomer’s Telegram, 900, 1
- Kuulkers, E., et al., 2006, The Astronomer’s Telegram, 888, 1
- Landolt, A. U., 1992, AJ, 104, 340
- Laycock, S., Zhao, P., Berg, M. V. D., Grindlay, J., & Hong, J., 2006, The Astronomer’s Telegram, 895, 1
- Markwardt, C. B., & Swank, J. H., 2006, The Astronomer’s Telegram, 891, 1
- Massey, P., & Davis, L. E., 1992, *A User’s Guide to Stellar CCD Photometry with IRAF*
- Paizis, A., Nowak, M. A., Rodriguez, J., Wilms, J., Courvoisier, T. J.-L., Del Santo, M., Ubertini, P., & Ebisawa, K., 2006, The Astronomer’s Telegram, 907, 1
- Persson, S. E., Murphy, D. C., Krzeminski, W., Roth, M., & Rieke, M. J., 1998, AJ, 116, 2475
- Predehl, P., & Schmitt, J. H. M. M., 1995, A&A, 293, 889
- Rieke, G. H., & Lebofsky, M. J., 1985, ApJ, 288, 618
- Rodriguez, J., Cadolle-Bel, M., Tomsick, J. A., Corbel, S., Procksopp, C., Paizis, A., Shaw, S., & Bodaghee, A., 2006, Submitted to ApJ
- Shaw, S., et al., 2006, The Astronomer’s Telegram, 886, 1
- Soldi, S., et al., 2006, The Astronomer’s Telegram, 885, 1
- Torres, M. A. P., Steeghs, D., Jonker, P. G., Burns, C. R., & Freedman, W. L., 2006, The Astronomer’s Telegram, 909, 1

Ubertini, P., et al., 2003, *A&A*, 411, L131
Wang, Q. D., et al., 2005, *ApJ*, 635, 386
Winkler, C., et al., 2003, *A&A*, 411, L1